Marine Chemistry 201 (2018) 256–262

Contents lists available at ScienceDirect

Marine Chemistry

journal homepage: www.elsevier.com/locate/marchem

# Biogeochemical cycling of Zn and Cd and their stable isotopes in the Eastern Tropical South Pacific

Seth G. John[a,b,*], Joshua Helgoe[a], Emily Townsend[a]

[a] Department of Earth and Ocean Sciences, University of South Carolina, Columbia, SC, United States
[b] Department of Earth Sciences, University of Southern California, Los Angeles, CA, United States

ARTICLE INFO

*Keywords:*
d66Zn
d114Cd
e112Cd
e114Cd

ABSTRACT

The distribution of Zn and Cd and their stable isotope ratios ($\delta^{66}$Zn and $\delta^{114}$Cd) were measured on samples from the Eastern Subtropical South Pacific Zonal Transect (EPZT), US GEOTRACES section GP16. The broad trends in both $\delta^{66}$Zn and $\delta^{114}$Cd are similar to those observed in other ocean basins, suggesting global similarities in the biogeochemical processes which cycle Zn and Cd. For example, average deep ocean $\delta^{66}$Zn along this transect (+0.46‰) are similar to the ~+0.5‰ values observed in the deep North Atlantic and North Pacific. Also similar to other locations, $\delta^{66}$Zn decreases towards the surface ocean. A plume of hydrothermal Zn emanating from the East Pacific Rise is used to calculate hydrothermal end-member $\delta^{66}$Zn as +0.24‰, which is similar to crustal values and similar to other sources of Zn to the oceans. Average deep-ocean $\delta^{114}$Cd along this transect is +0.28‰, which is similar to deep-ocean values between +0.2 and +0.3 measured elsewhere in the Atlantic, Pacific, and Southern Oceans. $\delta^{114}$Cd increases towards the surface ocean, as observed in other ocean basins, reflecting the preferential biological uptake of lighter Cd isotopes. Elsewhere it has been hypothesized that Cd can precipitate in sulfidic microenvironments on sinking particles, affecting seawater Cd concentrations and isotope ratios. However, we don't find evidence of particularly strong CdS precipitation along this transect, despite the fact that the Peru OMZ is one of the most reducing ocean environments worldwide.

## 1. Introduction

Zinc (Zn) and cadmium (Cd) are oceanographically important elements. Zn and Cd are both micronutrients necessary for the growth of phytoplankton in the ocean. Additionally, because Zn and Cd are biologically cycled they can be used to trace other important processes such as the uptake and remineralization of nutrients and biological material in the oceans. Zn and Cd stable isotopes ($\delta^{66}$Zn and $\delta^{114}$Cd) can provide insights into both these processes, helping us to understand how Zn and Cd are directly involved in biological processes in the oceans and serving as tracers for a variety of important marine biogeochemical processes.

Seawater dissolved $\delta^{66}$Zn has been measured in several major ocean basins, though never before in the South Pacific. In the deep ocean below ~1000 m, $\delta^{66}$Zn values similar to +0.5‰ have been observed in the Southern Ocean (Zhao et al., 2013), North Atlantic (Conway and John, 2014), and North Pacific (Conway and John, 2015b). This suggests a globally homogeneous deep-ocean $\delta^{66}$Zn even as Zn concentrations increase by roughly an order of magnitude from the high-latitude North Atlantic to the North Pacific. In the upper ocean, these same studies show decreasing $\delta^{66}$Zn towards the surface ocean in the North Atlantic and North Pacific, and little change in $\delta^{66}$Zn towards the surface in the Southern Ocean. The decrease in $\delta^{66}$Zn observed in the North Atlantic and North Pacific is at odds with culture experiments showing that phytoplankton in culture assimilate isotopically light Zn (John et al., 2007; John and Conway, 2013), which would be expected to leave the residual dissolved phase isotopically heavier. However, it has also been observed that Zn which adsorbs onto biological material is isotopically heavier than dissolved Zn in some conditions, leading to the suggestion that isotopically heavy Zn may be scavenged from the dissolved phase onto sinking biogenic material in the upper ocean (John and Conway, 2013).

Recently, using data from the GP16 transect reported here, Roshan et al. (2016) observed a significant long-range plume of hydrothermal Zn emanating from the East Pacific Rise and suggested that hydrothermal input may be the dominant source of Zn to the global oceans.

Seawater dissolved $\delta^{114}$Cd has been measured in many of the same locations as Zn. The global deep ocean $\delta^{114}$Cd is also relatively homogeneous throughout the global deep ocean near +0.3‰ (Ripperger et al., 2007; Abouchami et al., 2011; Xue et al., 2013; Conway and

* Corresponding author at: Department of Earth Sciences, University of Southern California, Los Angeles, CA, United States
*E-mail address:* sethjohn@usc.edu (S.G. John).

http://dx.doi.org/10.1016/j.marchem.2017.06.001
Received 5 January 2017; Received in revised form 14 March 2017; Accepted 2 June 2017
Available online 04 June 2017
0304-4203/ 

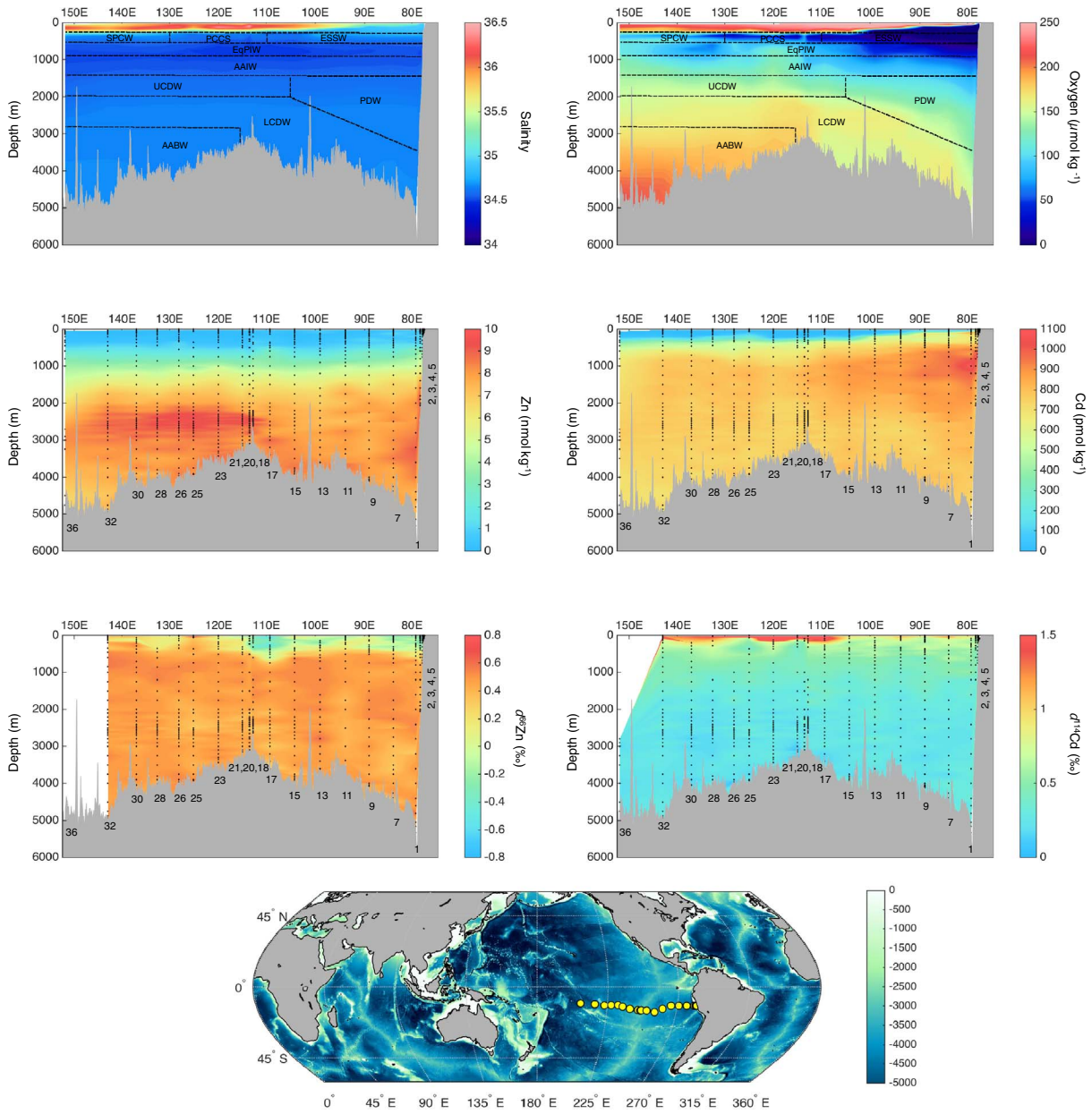


**Fig. 1.** Distribution of salinity, oxygen, Zn, Cd, $\delta^{66}$Zn and $\delta^{114}$Cd along the EPZT transect and map of station locations. Water mass distributions overlaid on salinity and oxygen plots delineate the regions dominated by various water masses based on Peters et al. (2017) and include Equatorial Subsurface Water (ESSW), South Pacific Central Water (SPCW), waters of the Peru-Chile Current System (PCCS), Equatorial Pacific Water (EqPW), Antarctic Intermediate Water (AAIW), Pacific Deep Water (PDW), Upper Circumpolar Deep Water (UCDW), Lower Circumpolar Deep Water (LCDW), and Antarctic Bottom Water (AABW).

John, 2015a, 2015b). The biological cycling of Cd isotopes in the upper ocean is more straightforward than Zn. $\delta^{114}$Cd generally increases monotonically towards the surface ocean, reflecting the preferential assimilation of lighter Cd isotopes by phytoplankton which has also been measured in culture (Lacan et al., 2006; John and Conway, 2013).

An intriguing wrinkle in the global Cd cycle is the suggestion that Cd may be precipitated as CdS within sulfidic microenvironments surrounding organic particles in OMZs. This has been inferred both from the relative depletion of Cd compared to P in OMZs (Janssen et al., 2014), and from the anomalously high dissolved $\delta^{114}$Cd values observed in the same waters which would be consistent with precipitation of isotopically light sulfides (Janssen et al., 2014; Conway and John, 2015a).

The US GEOTRACES GP16, sometimes referred to as the Eastern Pacific Zonal Transect (EPZT), provides a unique opportunity to study the cycling of Zn and Cd. In the eastern portion of the transect, upwelling of nutrient-rich waters along the Peru margin sustains high levels of phytoplankton productivity in the surface ocean (Bruland et al., 2005). Next to the Peru margin below the surface (~100–1000 m), slow ventilation of mid-depth waters combined with a high flux of organic carbon from the surface leads to the formation of an oxygen minimum zone (OMZ) which is one of the globes largest regions of denitrification (Lam et al., 2009). Conditions in the western portion of the transect are very different. Surface waters there are part of the South Pacific oligotrophic gyre, one of the lowest-productivity regions of the global ocean. In the deep ocean the cruise transect crossed the East Pacific Rise (EPR) hydrothermal vent field and followed the track of a long plume of hydrothermal 3He, Fe, and Mn (Resing et al., 2015; Fitzsimmons et al., 2017). Here we present new datasets of dissolved $\delta^{66}$Zn and $\delta^{114}$Cd along the GEOTRACES GP16 transect and describe key features of their distribution.

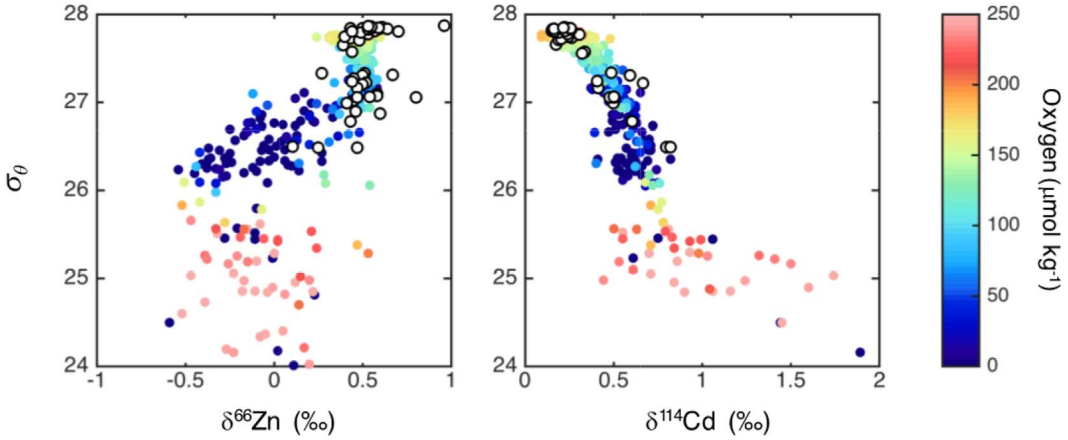


**Fig. 2.** Distribution of $\delta^{66}$Zn and $\delta^{114}$Cd compared to density along the EPZT (colored points), where coloring shows the EPZT oxygen concentrations of each sample with higher oxygen observed both in deep waters (highest $\sigma_\theta$) and surface waters (lowest $\sigma_\theta$). White circles represent surface data and profiles from the Southern Ocean (Abouchami et al., 2011; Xue et al., 2013; Zhao et al., 2013). (For interpretation of the references to color in this figure legend, the reader is referred to the web version of this article.)

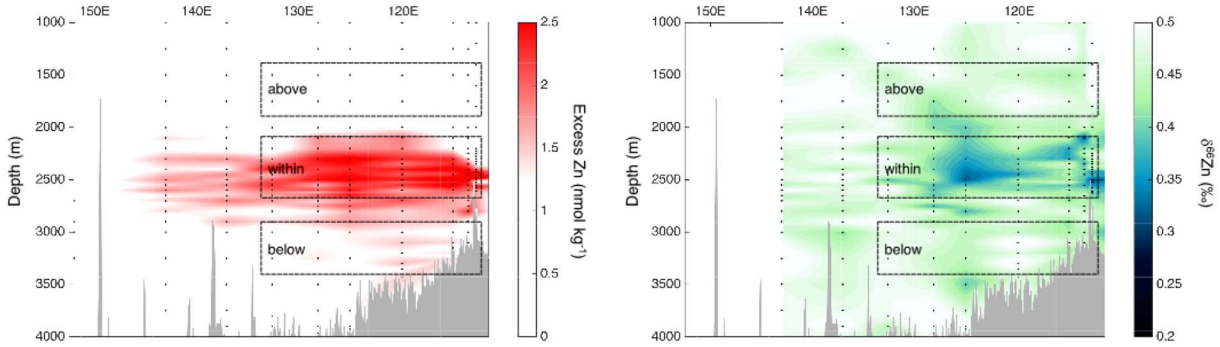


**Fig. 3.** Distribution of Zn* and $\delta^{66}$Zn within the hydrothermal plume. Boxes delineate the regions used to calculate background $\delta^{66}$Zn above and below the plume, and the region within the plume where Zn* is used to calculate hydrothermal end-member $\delta^{66}$Zn.

## 2. Methods

Samples were provided from the GEOTRACES trace-metal clean sampling rosette and were sampled through Acropak 0.2 µm capsule filters into acid-cleaned 1 L or 4 L LDPE bottles by the onboard GEOTRACES clean sampling team. When samples were received on shore they were acidified to pH 1.8 using clean hydrochloric acid and left at this pH for at least 3 months before processing.

A preliminary analysis of Fe, Zn, and Cd concentration was performed by a miniaturized version of the bulk extraction technique we use for isotope analyses. In a 15 mL centrifuge tube, 10 mL seawater samples were amended with 1 ng Fe double spike, 5 ng Zn double spike, 1 ng Cd double spike, 50 µL Nobias PA-1 resin, and adjusted to pH 5–7 with an ammonium acetate buffer. Samples were then loaded onto a PrepFast (Elemental Scientific Inc.) and processed according to a pre-programmed routine. Seawater was removed by suction into a PFA tube fitted with a small frit on the end so that resin remained in the vial, then this same tube was used three times to rinse the resin with 2 mL ultrapure water, and then 0.5 mL of 5% $HNO_3$ was added to the resin to release the metals. After sitting with the resin for at least 20 min, the 5% $HNO_3$ was suctioned off the resin by the PFA tube, and transferred to a new clean 15 mL vial. Samples were then analyzed on an Element ICPMS by isotope dilution using ratios of $^{57}Fe/^{56}Fe$, $^{67}Zn/^{66}Zn$, and $^{114}Cd/^{110}Cd$. Cd isotopes were corrected for interferences of $^{110}$Pd and $^{114}$Sn by analysis of $^{105}$Pd and $^{118}$Sn, and for $MoO^+$ by monitoring the formation of MoO in a Mo-amended seawater sample according to the procedure of Biller and Bruland (2012). These data are generally not included in our final dataset except in rare cases where the concentration data based on 1 L samples was not available, because we presume that the greater amount of analyte and greater precision of multi-collector ICP-MS leads to higher quality concentration data from large volume samples.

Large volume (1 L) seawater samples were processed and analyzed for [Zn], [Cd], $\delta^{66}$Zn and $\delta^{114}$Cd according to previously published methods (Conway et al., 2013). Briefly, Fe, Zn, and Cd double-spikes were added to the acidified samples and allowed to equilibrate for > 1 h. Metals were then extracted from seawater onto an ethylenediaminetriacetic acid resin (Nobias PA-1; Hitachi) for 2 h at pH 2 and 2 h at pH between 6 and 6.3. Metals were eluted off this resin using 3 N $HNO_3$, and were then purified by anion exchange chromatography before being reconstituted in 0.1 N $HNO_3$ for analysis. Concentrations and stable isotope ratios were determined simultaneously by analysis on a Neptune multi-collector ICP-MS. Zn was analyzed in high resolution mode and Cd was analyzed in low resolution mode. Instrumental and procedural isotope fractionation was corrected for using a double-spike data reduction scheme. Concentrations were calculated using isotope-dilution to calculate ng of metal per sample, and then converted to nmol $kg^{-1}$ or pmol $kg^{-1}$ using the weight of each sample processed. The largest sources of error for concentration analyses are determining the weight of the sample and determining the volume of double-spike added to each sample. We approximate 5% error for each sample based on the combination of these two factors. Accuracy was checked by analysis of S, D1 and D2 SAFe reference standards (for which we determined values identical to the consensus values; see Conway et al., 2013) and inter-comparison with two other groups measuring trace metal concentrations on GP16 samples.

Data are plotted using an in-house Matlab routine which first linearly interpolates data at each station in the vertical direction, then interpolates horizontally between stations. This method therefore plots the true measured value at each point where a sample was collected, in

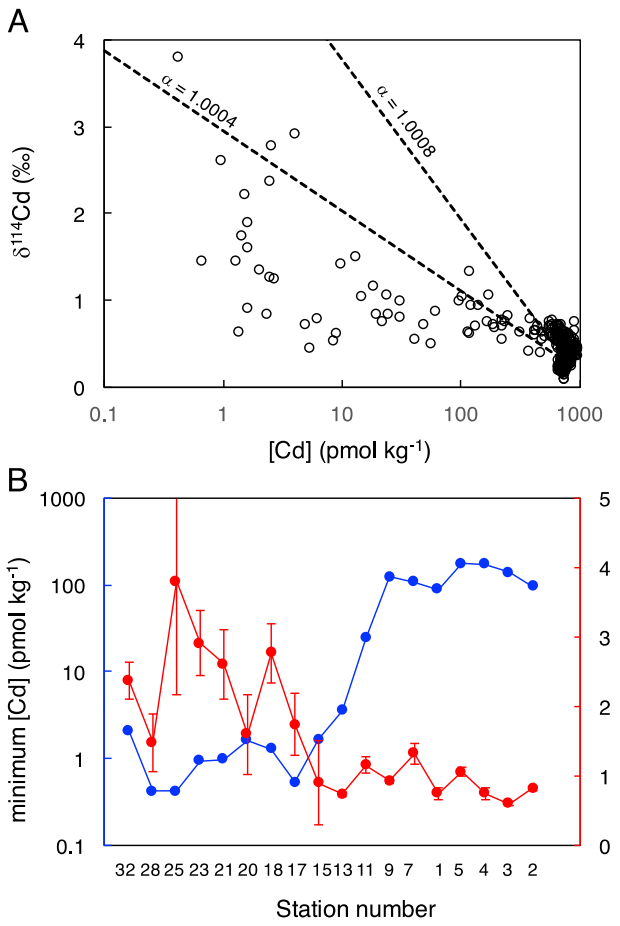


**Fig. 4.** Surface minimum Cd concentrations and maximum $\delta^{114}$Cd from stations across the transect demonstrate an increase in $\delta^{114}$Cd at roughly the same location where Cd declines to ~1 pmol kg$^{-1}$ (A). The relationship between Cd and $\delta^{114}$Cd for all samples shows that highest $\delta^{114}$Cd values are associated with lower [Cd], though there is significant departure from Rayleigh fractionation lines (dashed lines) which is likely attributed to mixing (B).

contrast to other popular schemes which may not plot the true value of points which appear to be 'flyers' with respect to other nearby data.

All of the data are currently available through the Biological and Chemical Oceanography Data Management Office (BCO-DMO) website, and will eventually be included in the GEOTRACES 2017 Intermediate Data Product.

## 3. Results and discussion

### 3.1. Intercalibration and error

Each full-depth profile along the transect included two 'crossover-depths' which were sampled on different casts of the GEOTRACES rosette. This sampling strategy was undertaken in order to provide a means for methods intercalibration, which is required for all GEOTRACES cruises but for which there were no crossover stations on this transect. Additionally, this provides a unique opportunity to quantify the error in our analyses. Early testing of the method used here suggested that the main source of error in analyses of $\delta^{56}$Fe, $\delta^{66}$Zn, and $\delta^{114}$Cd was internal analytical error, which was in turn comprised of error from counting statistics, Johnson noise, and plasma flicker (John, 2012; Conway et al., 2013). However, more recent work indicates that there are additional sources of error, at least for $\delta^{66}$Zn. For example, the intermediate error (error when the same sample is run during different analytical sessions) can be assessed whenever a large number of samples are re-analyzed during two or more different analytical sessions (John and Adkins, 2010; John, 2012). For samples with > 0.4 nM Zn from the North Atlantic GEOTRACES transect, intermediate error was 0.05‰ (2σ, $n$ = 30), or roughly twice the internal error (T. Conway, personal communication).

Here we determine the relationship between internal error and external reproducibility from the population of error normalized deviates (END, similar to the $t$-statistic) for all crossover depths according to methods previously used for Fe isotopes (John and Adkins, 2010; John, 2012). For $\delta^{66}$Zn we find that the standard deviation for all END values is 3.26 ($n$ = 26), meaning that the external reproducibility including all sources of error is roughly three times the internal error. External error cannot be attributed to variations in water mass $\delta^{66}$Zn because the deep ocean is well-mixed with respect to $\delta^{66}$Zn and crossover-depth samples were taken within several m vertically and several km horizontally from each other. The larger error also cannot be attributed to sample contamination because there is no clear relationship between $\delta^{66}$Zn and higher or lower [Zn]. A plausible explanation for the external error observed here is the presence of a minor polyatomic interference during mass-spectrometry analysis such as $^{40}Ar^{27}Si^{+}$, $^{132}Ba^{++}$, $^{134}Ba^{++}$, $^{136}Ba^{++}$, or $^{40}Ar^{14}N_2^{+}$. This would be consistent with a change in the magnitude of external error between various studies (e.g. between this transect and data from the US GEOTRACES North Atlantic transect), if there are systematic changes in the amount of polyatomic interference due to either slight changes in technique with different experimentalists or changes in instrument function over time. Even with this larger error there is still sufficient accuracy to resolve large-scale patterns in seawater $\delta^{66}$Zn. For example, assuming that true external error is three

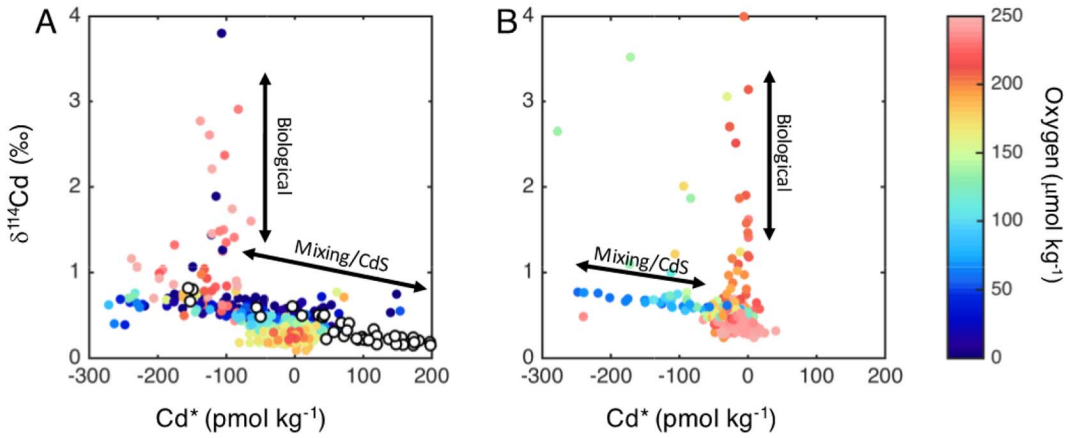


**Fig. 5.** The relationship between $\delta^{114}$Cd and Cd* along the EPZT transect (A) compared to data from the North Atlantic GA03 transect (B) (Conway and John, 2015a). White points are data from profiles in the Southern Ocean (Abouchami et al., 2011; Xue et al., 2013). Arrow represent the changes in Cd* and $\delta^{114}$Cd expected for biological uptake and remineralization of Cd (Biological) and for mixing of water masses and/or CdS precipitation and dissolution (Mixing/CdS).

times internal error for our dataset would result in an average external error of only 0.09‰ (2σ) for deep-ocean samples (> 1000 m).

The external error for $\delta^{114}$Cd is more similar to internal error. Following the same approach as outlined above for $\delta^{66}$Zn, we find that external error is 1.31 times greater than internal error. In the deep ocean this would correspond to an average error of 0.05‰ (2σ), which is sufficient to resolve large-scale patterns in $\delta^{114}$Cd.

In order to apply the most conservative estimate of error, we therefore report 3.26 times internal error for $\delta^{66}$Zn and 1.31 times internal error for $\delta^{114}$Cd for all data from the EPZT transect.

### 3.2. Zn and $\delta^{66}$Zn

The broad patterns in $\delta^{66}$Zn observed along the EPZT transect are similar to those previously observed in the North Atlantic, Southern Ocean, and North Pacific. $\delta^{66}$Zn is relatively homogeneous below ~1000 m (Fig. 1). The average $\delta^{66}$Zn below 1000 m for this transect in the South Pacific is +0.46 ± 0.05‰ (1σ SD), similar to the global mean $\delta^{66}$Zn of +0.50 ± 0.14‰ calculated by Conway and John (2015b). As seen in other parts of the ocean including the Atlantic and North Pacific, $\delta^{66}$Zn often decreases towards the surface ocean. Interestingly, the magnitude of the decrease in $\delta^{66}$Zn is larger in the eastern portion of the transect (Stn 1–21; −0.01 ± 0.30‰, 1σ SD) compared to the western portion of the transect (Stn 23–32; +0.37 ± 0.19‰, 1σ SD). There is no clear change in Zn concentrations at this transition point, however it does align roughly with the transition in subsurface water masses from ESSW in the east to SPCW and PCCS in the west. Both of the eastern water masses move northwards from their origination at more southern latitudes, while ESSW originates at the equator and moves southwards (Peters et al., 2017). This suggests some difference in Zn isotope fractionation between the tropical surface waters to the north and the subtropical/temperate ocean regions to the south. For example, there might be a difference in the amount of Zn removed by biological uptake compared to scavenging onto sinking organic particles. Or perhaps there is a difference in the isotope effect during Zn removal, either due to differences in the characteristics of particles onto which Zn is adsorbing or to differences in Zn isotope fractionation by different phytoplankton species which predominate in tropical compared to subtropical/temperate regions. Finally, the difference could be attributed to a greater degree of mixing between SPCW/PCCS waters and the underlying Equatorial Pacific Water (EqPW). During mixing of water masses the isotope signature of the water mass with higher concentrations will tend to erase the signature of the low-concentration water mass, for example higher Zn concentrations in EqPW with a $\delta^{66}$Zn signature near ~+0.5‰ may be mixing with Zn-depleted SPCW/PCCS and imparting their heavier $\delta^{66}$Zn signature. This transition in $\delta^{66}$Zn values coincides roughly with a change in surface-ocean [Cd] and $\delta^{114}$Cd, again pointing to differences in the character or magnitude of upper-ocean biological processes which influence the water masses observed in the eastern and western portions of the transect.

The processes which fractionate Zn isotopes in the ocean interior can be further studied by comparing our data with samples collected along the same isopycnals in the Southern Ocean where they outcrop at the surface (Fig. 2). Because EPZT waters mix with Southern Ocean waters along isopycnals, we would expect waters with the same density to have similar properties (e.g. [Zn] and $\delta^{66}$Zn) in the EPZT and the Southern Ocean if their distribution were controlled only by mixing. Conversely, dissimilarities can point to active biogeochemical cycling of Zn as waters move between these two regions. Southern Ocean $\delta^{66}$Zn are taken from a surface transect and four depth profiles in the Southern Ocean (Zhao et al., 2013). Comparing $\delta^{66}$Zn to potential density ($\sigma_\theta$) for both datasets, we see that $\delta^{66}$Zn in both datasets is similar to +0.5‰ for deep ocean samples ($\sigma_\theta > 27$). In less dense waters ($26 < \sigma_\theta < 27$), however, the average Southern Ocean $\delta^{66}$Zn does not change much while the average $\delta^{66}$Zn of EPZT samples decreases to roughly −0.25‰ at $\sigma_\theta = 26$. These waters are mostly in the core of the OMZ ($[O_2] < \sim 50\ \mu mol\ kg^{-1}$), suggesting a process which preferentially removes heavier Zn isotopes. Sulfide precipitation has been hypothesized to remove dissolved Zn from OMZ waters (Janssen et al., 2014), but sulfide precipitation is known to preferentially remove lighter Zn isotopes based on laboratory, hydrothermal vent, and observational studies in euxinic basins (Archer et al., 2004; Mason et al., 2005; John et al., 2008; Vance et al., 2016). Instead, we propose the most likely explanation is preferential scavenging of isotopically heavy Zn onto particles sinking through the OMZ. In upper-ocean waters ($\sigma_\theta < 26$) we don't see a dramatic change in $\delta^{66}$Zn, suggesting that Zn isotopes are not greatly fractionated by biological cycling in the surface ocean. While a lack of biological Zn isotope fractionation is at odds with culture data, it is consistent with the finding that $\delta^{66}$Zn does not greatly change in the surface Southern Ocean or Black Sea even while Zn is greatly depleted by biological uptake (Zhao et al., 2013; Vance et al., 2016).

A unique feature of the EPZT transect is the discovery of a hydrothermal Zn plume (Roshan et al., 2016). This plume is observable from the Zn concentration data alone, and it becomes even more noticeable after subtracting away the contribution of 'nutrient-type' Zn by calculating Zn* ($Zn^* = Zn - 0.053 \cdot Si$), based on the global similarity between ocean Zn and Si concentrations (Fig. 3). While the feature does not stand out in the $\delta^{66}$Zn data when plotting the entire transect (Fig. 1), a close examination shows that there is a slight decrease in the average $\delta^{66}$Zn within the plume (Fig. 3). In order to quantitatively constrain the $\delta^{66}$Zn of hydrothermal input, we compare Zn* and $\delta^{66}$Zn within the core of the plume (2200–3000 m; stations 20 to 34) to 'background' regions above and below the plume (1500–2000 m and 3000–3500 m, respectively). Above and below the plume we calculate average $\delta^{66}$Zn of +0.48 ± 0.010‰ and +0.47 ± 0.007‰ (1σ SE, $n = 14$ and $n = 25$, respectively). The average $\delta^{66}$Zn within the plume is lighter with an average value of +0.42 ± 0.006‰ (1σ SE, $n = 65$). Assuming that the average $\delta^{66}$Zn values from above and below the plume represent the non-hydrothermal background $\delta^{66}$Zn, and that Zn* represents the quantity of hydrothermal Zn within the plume, we can then solve for the $\delta^{66}$Zn of the hydrothermal end-member using a least-squares approach to minimizing the misfit between predicted and observed plume $\delta^{66}$Zn. Using this technique we calculate a hydrothermal $\delta^{66}$Zn of +0.24 ± 0.06‰ (1σ SE). The total range of $\delta^{66}$Zn measured in pure hydrothermal fluids ranges widely from 0.00‰ to +1.33‰ (John et al., 2008), and a $\delta^{66}$Zn of −0.5‰ was inferred for pure fluids from the TAG vent field on the Mid-Atlantic Rise (Conway and John, 2014). However, our calculated end-member value nicely matches the concentration-weighted mean $\delta^{66}$Zn of EPR hydrothermal fluids of +0.24‰ (John et al., 2008; Little et al., 2014). Overall, our data suggest hydrothermal $\delta^{66}$Zn is within the range measured for lithogenic materials (+0.31 ± 0.11‰), and therefore it has a similar Zn isotope composition as other important sources of Zn to the oceans (Little et al., 2014, 2016).

The reason for different a much higher hydrothermal end-member $\delta^{66}$Zn in EPR fluids compared to TAG fluids is not fully understood. Presumably subsurface hydrothermal fluids acquire a $\delta^{66}$Zn similar to basalt and other lithogenic materials as they travel through the seafloor (~+0.3‰). This suggests that Zn in EPR fluids is not isotopically fractionated during mixing with seawater, while isotopically heavier Zn is preferentially lost from TAG fluids during mixing. Perhaps this can be attributed to the lower $Fe/H_2S$ ratios in TAG fluids, which favors quantitative precipitation of the available sulfide by Fe, leaving some of the Zn uncomplexed by sulfide and susceptible to scavenging onto Fe oxyhydroxides (Edmonds and German, 2004; Severmann et al., 2004; John et al., 2008), a process which has previously been shown to remove heavier Zn isotopes (John et al., 2007). Similarly, it could be that high sulfide concentrations in EPR fluids lead to quantitative precipitation of ZnS so that it maintains the same $\delta^{66}$Zn as the original subsurface fluids. If so, this would suggest that the dissolved form of Zn is as nanoparticulate sulfides as previously hypothesized for Fe (Yucel

et al., 2011), or that it originated as nanoparticulate sulfide Zn which subsequently dissolved as the plume traversed the deep Pacific.

### 3.3. Cd and $\delta^{114}Cd$

Cadmium concentrations and stable isotopes show the same broad patterns along the EPZT as observed in other ocean basins. Along the EPZT below 1000 m the average $\delta^{114}Cd$ is $+0.28 \pm 0.07$‰ (1σ SD), similar to previously-measured deep ocean values between +0.2 to +0.3‰ (Ripperger et al., 2007; Abouchami et al., 2011, 2014; Boyle et al., 2012; Yang et al., 2012; Xue et al., 2013; Conway and John, 2015a, 2015b). $\delta^{114}Cd$ increases towards the surface ocean, presumably reflecting the biological preference for uptake of lighter Cd isotopes by phytoplankton. EPZT dissolved seawater $\delta^{114}Cd$ values do not lie along a single Rayleigh mass fractionation line, presumably because even if biological Cd uptake is defined by a single fractionation factor, this signal is complicated by mixing between higher-Cd and lower-Cd waters which produces $\delta^{114}Cd$ values lower than would be predicted for Rayleigh distillation (Fig. 4). The most fractionated samples lie near the $\alpha = 1.0004$ fractionation line, which is similar to the biological fractionations observed in the Antarctic Circumpolar Current ($\alpha = 1.0002$ for $\varepsilon^{112/110}Cd$) (Abouchami et al., 2014). All samples are well below the line for the $\alpha = 1.0008$ fractionation observed in culture (Lacan et al., 2006; John and Conway, 2013), suggesting that natural phytoplankton fractionate Cd isotopes less than those growing in culture. Values below this Rayleigh distillation line may be attributed to mixing of waters with different Cd concentrations, which always produces $\delta^{114}Cd$ values lower than Rayleigh distillation because the Cd in mixed waters is dominated by the higher Cd concentrations in less-fractionated waters. The heaviest $\delta^{114}Cd$ values are observed in surface waters in the western portion of the transect (west of 105°E, stations 17 to 32). This corresponds to a deeper nutricline (Fig. 1) and a decrease in surface minimum [Cd] to about 1 pmol $kg^{-1}$ (Fig. 4).

We don't find evidence of extraordinarily large amounts of Cd sulfide precipitation along the EPZT, despite the Peruvian oxygen minimum zone (OMZ) being one of the most intensely reducing environments worldwide. Oxygen is depleted below detectable limits throughout the core of the OMZ, and it is one of the most globally important sites of denitrification (Lam et al., 2009). While the OMZ is not euxinic (there are no detectable levels of sulfide in the water column), it has been proposed as an important region where sulfide might be generated within organic particles as part of the so called 'cryptic sulfur cycle' (Canfield et al., 2010). In contrast, regions where CdS precipitation has been hypothesized such as the North Pacific (Janssen et al., 2014) and North Atlantic (Conway and John, 2015a) have much higher oxygen concentrations (minimum $[O_2]$ of ~50 and ~150 μmol $kg^{-1}$, respectively). One tracer for possible CdS precipitation is Cd*, or the relative loss of Cd compared to P where:

$$Cd^* = Cd_{measured} - (Cd/P_{deep} \cdot P_{measured}) \quad (1)$$

Here, we use a $Cd/P_{deep}$ of 250 (pM/μM) as was used for the North Atlantic (Janssen et al., 2014), since global Cd/P is mostly similar throughout the global deep ocean despite small inter-basin differences (Löscher et al., 1997). Compared to the North Atlantic GEOTRACES transect, levels of Cd depletion as measured from Cd* are not any greater despite the much lower oxygen concentrations along the EPZT (Fig. 5). Furthermore, two key features of the EPZT data which might otherwise be attributed to CdS precipitation are also found in the Southern Ocean. First, the increase in $\delta^{114}Cd$ at low oxygen concentrations is also apparent in Southern Ocean waters at the same isopycnal, despite much greater oxygen concentrations in the Southern Ocean where waters are in closer contact with the atmosphere (Fig. 2). Secondly, the lower Cd* observed in low-oxygen EPZT waters is also observed in the Southern Ocean, again suggesting that this signal could be caused by the uptake of Cd and P by phytoplankton in the surface Southern Ocean, rather than CdS precipitation in the OMZ (Fig. 5). It is difficult to know exactly where these signals originate, as waters exchange back and forth between the Southern Ocean and EPZT. It may be that some amount of CdS precipitation does occur, even if evidence suggests that this process is not dramatically stronger in the Peru Upwelling OMZ compared to other less oxygen-depleted regimes.

## 4. Conclusions

Our new data on $\delta^{66}Zn$ and $\delta^{114}Cd$ is part of an ever-growing database of seawater trace-element concentrations and stable isotope ratios in the global oceans generated by GEOTRACES and other programs. The overall patterns in both $\delta^{66}Zn$ and $\delta^{114}Cd$ are similar to patterns seen in other ocean basins, suggesting that the first-order controls on Zn and Cd isotope biogeochemical cycling are globally similar. However, unique features were also observed along the EPZT such as the hydrothermal Zn plume, the abrupt change in upper-ocean $\delta^{66}Zn$ in the middle of the transect, and the lack of dramatic Cd* and $\delta^{114}Cd$ changes within the OMZ. We anticipate that future studies will incorporate our data with other large-scale datasets from around the globe, leading to more discoveries and a better understanding of the global biogeochemical cycling of these important elements.

## Acknowledgements

Thanks to the captain and crew of the R/V *Thomas Thompson*, GP16 chief scientists J. Moffett and C. German, and especially to the sampling team who collected all of our dissolved samples at sea including Claire Till, Cheryl Zurbrick, and Geoffrey Smith. This work was supported by NSF Chemical Oceanography grant 1235150.

## References

Abouchami, W., Galer, S.J.G., de Baar, H.J.W., Alderkamp, A.C., Middag, R., Laan, P., Feldmann, H., Andreae, M.O., 2011. Modulation of the Southern Ocean cadmium isotope signature by ocean circulation and primary productivity. Earth Planet. Sci. Lett. 305, 83–91.

Abouchami, W., Galer, S.J.G., de Baar, H.J.W., Middag, R., Vance, D., Zhao, Y., Klunder, M., Mezger, K., Feldmann, H., Andreae, M.O., 2014. Biogeochemical cycling of cadmium isotopes in the Southern Ocean along the Zero Meridian. Geochim. Cosmochim. Acta 127, 348–367.

Archer, C., Vance, D., Butler, I., 2004. Abiotic Zn isotope fractionations associated with ZnS precipitation. Geochim. Cosmochim. Acta 68, A325.

Biller, D.V., Bruland, K.W., 2012. Analysis of Mn, Fe, Co, Ni, Cu, Zn, Cd, and Pb in seawater using the Nobias-chelate PA1 resin and magnetic sector inductively coupled plasma mass spectrometry (ICP-MS). Mar. Chem. 130–131, 12–20.

Boyle, E.A., John, S.G., Abouchami, W., Adkins, J.F., Echegoyen-Sanz, Y., Ellwood, M., Flegal, A.R., Fornace, K., Gallon, C., Galer, S.J.G., et al., 2012. GEOTRACES IC1 (BATS) contamination-prone trace element isotopes Cd, Fe, Pb, Zn, Cu, and Mo intercalibration. Limnol. Oceanogr. Methods 10, 653–665.

Bruland, K.W., Rue, E.L., Smith, G.J., DiTullio, G.R., 2005. Iron, macronutrients and diatom blooms in the Peru upwelling regime: brown and blue waters of Peru. Mar. Chem. 93, 81–103.

Canfield, D.E., Stewart, F.J., Thamdrup, B., De Brabandere, L., Dalsgaard, T., Delong, E.F., Revsbech, N.P., Ulloa, O., 2010. A cryptic sulfur cycle in oxygen-minimum-zone waters off the Chilean Coast. Science 330, 1375–1378.

Conway, T.M., John, S.G., 2014. The biogeochemical cycling of zinc and zinc isotopes in the North Atlantic Ocean. Glob. Biogeochem. Cycles 28, 1111–1128.

Conway, T.M., John, S.G., 2015a. Biogeochemical cycling of cadmium isotopes along a high-resolution section through the North Atlantic Ocean. Geochim. Cosmochim. Acta 148, 269–283.

Conway, T.M., John, S.G., 2015b. The cycling of iron, zinc and cadmium in the North East Pacific Ocean - insights from stable isotopes. Geochim. Cosmochim. Acta 164, 262–283.

Conway, T.M., Rosenberg, A.D., Adkins, J.F., John, S.G., 2013. A new method for precise determination of iron, zinc and cadmium stable isotope ratios in seawater by double-spike mass spectrometry. Anal. Chim. Acta 793, 44–52.

Edmonds, H.N., German, C.R., 2004. Particle geochemistry in the Rainbow hydrothermal plume, Mid-Atlantic Ridge. Geochim. Cosmochim. Acta 68, 759–772.

Fitzsimmons, J.N., John, S.G., Marsay, C.M., Hoffman, C.L., Nicholas, S.L., Toner, B.M., German, C.R., Sherrel, R.M., 2017. Iron persistence in a distal hydrothermal plume supported by dissolved-particulate exchange. Nat. Geosci 10, 195–201.

Janssen, D.J., Conway, T.M., John, S.G., Christian, J.R., Kramer, D.I., Pedersen, T.F., Cullen, J.T., 2014. Undocumented water column sink for cadmium in open ocean oxygen-deficient zones. Proc. Natl. Acad. Sci. U. S. A. 111, 6888–6893.

John, S.G., 2012. Optimizing sample and spike concentrations for isotopic analysis by double-spike ICPMS. J. Anal. At. Spectrom. 27, 2123.

John, S.G., Adkins, J.F., 2010. Analysis of dissolved iron isotopes in seawater. Mar. Chem. 119, 65–76.
John, S.G., Conway, T.M., 2013. A role for scavenging in the marine biogeochemical cycling of zinc and zinc isotopes. Earth Planet. Sci. Lett. 394, 159–167.
John, S.G., Geis, R.W., Saito, M.A., Boyle, E.A., 2007. Zinc isotope fractionation during high-affinity and low-affinity zinc transport by the marine diatom *Thalassiosira oceanica*. Limnol. Oceanogr. 52, 2710–2714.
John, S.G., Rouxel, O.J., Craddock, P.R., Engwall, A.M., Boyle, E.a., 2008. Zinc stable isotopes in seafloor hydrothermal vent fluids and chimneys. Earth Planet. Sci. Lett. 269, 17–28.
Lacan, F., Francois, R., Ji, Y.C., Sherrell, R.M., 2006. Cadmium isotopic composition in the ocean. Geochim. Cosmochim. Acta 70, 5104–5118.
Lam, P., Lavik, G., Jensen, M.M., van de Vossenberg, J., Schmid, M., Woebken, D., Dimitri, G., Amann, R., Jetten, M.S.M., Kuypers, M.M.M., 2009. Revising the nitrogen cycle in the Peruvian oxygen minimum zone. Proc. Natl. Acad. Sci. U. S. A. 106, 4752–4757.
Little, S.H., Vance, D., Walker-Brown, C., Landing, W.M., 2014. The oceanic mass balance of copper and zinc isotopes, investigated by analysis of their inputs, and outputs to ferromanganese oxide sediments. Geochim. Cosmochim. Acta 125, 673–693.
Little, S.H., Vance, D., McManus, J., Severmann, S., 2016. Key role of continental margin sediments in the oceanic mass balance of Zn and Zn isotopes. Geology 44, 207–210.
Löscher, B.M., van der Meer, J., de Baar, H.J.W., Saager, P.M., de Jong, J.T.M., 1997. The global Cd/phosphate relationship in deep ocean waters and the need for accuracy. Mar. Chem. 59, 87–93.
Mason, T.F.D., Weiss, D.J., Chapman, J.B., Wilkinson, J.J., Tessalina, S.G., Spiro, B., Horstwood, M.S.A., Spratt, J., Coles, B.J., 2005. Zn and Cu isotopic variability in the Alexandrinka volcanic-hosted massive sulphide (VHMS) ore deposit, Urals, Russia. Chem. Geol. 221, 170–187.
Peters, B.D., Casciotti, K., Jenkins, W.J., Swift, J.H., German, C.R., Moffett, J.W., Cutter, G.A., Brzezinski, M.A., 2017. Water mass analysis of the 2013 US GEOTRACES Eastern Pacific Zonal Transect. Mar. Chem (in press).
Resing, J.A., Sedwick, P.N., German, C.R., Jenkins, W.J., Moffett, J.W., Sohst, B.M., Tagliabue, A., 2015. Basin-scale transport of hydrothermal dissolved metals across the South Pacific Ocean. Nature 523, 200–203.
Ripperger, S., Rehamper, M., Porcelli, D., Halliday, A., 2007. Cadmium isotope fractionation in seawater - a signature of biological activity. Earth Planet. Sci. Lett. 261, 670–684.
Roshan, S., Wu, J., Jenkins, W.J., 2016. Long-range transport of hydrothermal dissolved Zn in the tropical South Pacific. Mar. Chem. 183, 25–32.
Severmann, S., Johnson, C.M., Beard, B.L., German, C.R., Edmonds, H.N., Chiba, H., Green, D.R.H., 2004. The effect of plume processes on the Fe isotope composition of hydrothermally derived Fe in the deep ocean as inferred from the Rainbow vent site, Mid-Atlantic Ridge, 36°14′N. Earth Planet. Sci. Lett. 225, 63–76.
Vance, D., Little, S.H., Archer, C., Cameron, V., Andersen, M.B., Rijkenberg, M.J.A., Lyons, T.W., 2016. The oceanic budgets of nickel and zinc isotopes: the importance of sulfidic environments as illustrated by the Black Sea. Philos. Trans. R. Soc. Lond. A Math. Phys. Eng. Sci. 374.
Xue, Z., Rehkämper, M., Horner, T.J., Abouchami, W., Middag, R., van de Flierd, T., de Baar, H.J.W., 2013. Cadmium isotope variations in the Southern Ocean. Earth Planet. Sci. Lett. 382, 161–172.
Yang, S.-C., Lee, D.-C., Ho, T.-Y., 2012. The isotopic composition of Cadmium in the water column of the South China Sea. Geochim. Cosmochim. Acta 98, 66–77.
Yucel, M., Gartman, A., Chan, C.S., Luther, G., 2011. Hydrothermal vents as a kinetically stable source of iron-sulphide-bearing nanoparticles to the ocean. Nat. Geosci. 4, 367–371.
Zhao, Y., Vance, D., Abouchami, W., de Baar, H.J.W., 2013. Biogeochemical cycling of zinc and its isotopes in the Southern Ocean. Geochim. Cosmochim. Acta 125, 653–672.